OSA CONTINUUM

# Electromagnetically induced transparency (EIT) amplitude noise spectroscopy

Ben Whitenack,[1] Devan Tormey,[1] Michael Crescimanno,[2] Andrew C. Funk,[1,*] and Shannon O'Leary[1]

[1] Department of Physics, Lewis & Clark College, Portland, OR 97219, USA
[2] Department of Physics and Astronomy, Youngstown State University, Youngstown, OH 44555-2001, USA
[*] andrewfunk@lclark.edu

**Abstract:** Intensity noise cross-correlation of the polarization eigenstates of light emerging from an atomic vapor cell in the Hanle EIT configuration results in high resolution spectroscopy even with free-running semiconductor lasers. We show that the character of the observed intensity noise in any output polarization basis can be modeled as a Markov process in the input light fields' amplitudes that excite the response of a three-level medium. This method has promise as an inexpensive and simpler approach to vector magnetometry and has applications in timekeeping and as a probe of dynamics of atomic coherence in warm vapor cells.



## 1. Introduction

Electromagnetically induced transparency (EIT) is a coherent multiphoton effect that results in an optical medium that would normally absorb light becoming "transparent" (i.e. being much less absorbing) [1]. EIT occurs due to quantum interference between the atomic transition pathways that couple to the optical fields. The optical frequency dependence of the quantum interference required for EIT, makes this process potentially useful for precision spectroscopic applications such as clocks, magnetometers, communication schemes, and quantum computation [2–7].

If the optical fields used for an EIT experiment have narrow frequency spectra (< 1 MHz), as is typical in a setup utilizing an external cavity diode laser (ECDL), it is relatively straight-forward to understand EIT and the fluctuations in the light after it has interacted with the medium by using a three level Lambda scheme model which is illustrated in Fig. 1(b). In this case we treat the light as classical single mode field and then calculate/measure the relevant properties of the light after exiting the medium [8–13]. Less coherent sources, such as the generic free running semiconductor laser diode used in this experiment, have broad frequency spectra (≈ 80 MHz) and the resulting EIT atom-light interaction is not well modeled in terms of polarization states of a single optical mode. This is also indicated by the low EIT contrast in our experiments.

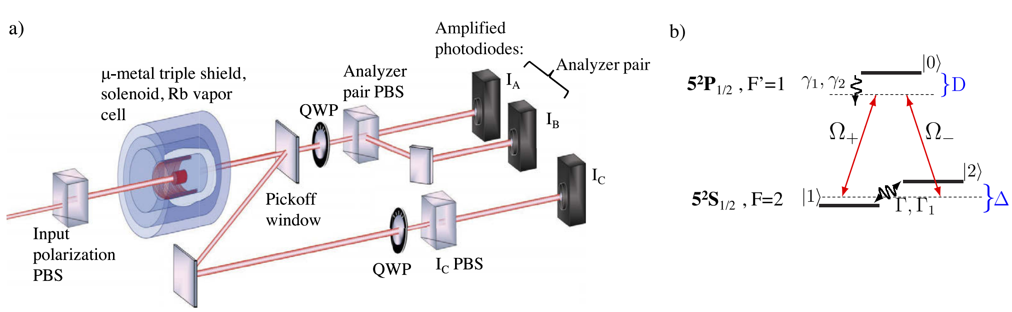


**Fig. 1.** (a) Experimental setup and (b) the 3-level diagram of the minimal atomic quantum optics model of EIT.

#384540 https://doi.org/10.1364/OSAC.384540
Journal © 2020 Received 10 Dec 2019; revised 10 Jan 2020; accepted 13 Jan 2020; published 4 Feb 2020

EIT intensity noise correlation spectra can be well modeled with a theory based on a reduced number of optical modes and are interesting spectroscopic probes [8–13]. They are understood as examples of the more general process of phase noise to amplitude noise conversion in atomic systems [14,15]. Here we present experimental results that test a reduced mode theory for any EIT intensity noise correlations arising chiefly from atom-light induced Markov process in the light field phases.

The use of a free-running diode laser to observe the intensity noise correlations in the light from EIT has technological relevance. A free-running diode laser is far less expensive and more mechanically robust than an ECDL. The broad optical spectrum of the free-running diode laser is advantageous here as the intensity noise correlations from EIT scale with the laser bandwidth. Furthermore, the use of (phase-)noisy lasers [16] may enjoy metrological advantages over other approaches since they can operate in a regime with good signal to noise but without power broadening [11,12,17–25].

Previous work studying the noise spectra of atomic systems has used the normalized intensity cross-correlation measure $g^{(2)}(0)$ to characterize and quantify the noise correlations in the atomic systems [16,17,23]. The intensity cross-correlation $g^{(2)}(0)$ is given by:

$$g^{(2)}(0) = \frac{\langle(\delta I_a)\,(\delta I_b)\rangle}{\sqrt{\langle(\delta I_a)^2\rangle\langle(\,\delta I_b)^2\rangle}}, \tag{1}$$

where $\delta I_{a(b)}$ is the intensity fluctuation for an optical mode $a(b)$, with $\delta I_a = I_a - \langle I_a\rangle$. Previous work has considered only the intensity noise correlation between the eigenmodes of the EIT process. In the case of Hanle EIT, the eigenmodes are the left and right hand circular polarizations of the incident laser light. Using $g^{(2)}(0)$ with the system's eigenmodes as the spectroscopic measure for an atomic system is useful if any changes to the system occur only in terms of the eigenmodes. For example, a magnetic field that is aligned along the direction of the laser propagation affects only the optical eigenmodes. Using only $g^{(2)}(0)$ as shown above gives information about the intensity noise of the two eigenmodes and how the intensity noise of those two modes is correlated. However it does not provide information about the amplitude noise of the optical modes [11,16,20]. By amplitude noise we mean the fluctuations in both the magnitude and relative phase of an optical mode (where the phase is relative to the other specified mode $a$ or $b$). As mentioned above, in the case that one wants the spectrum of the system as a function of a perturbation that occurs colinearly with the laser propagation direction, the noise information is entirely in the intensities of the eigenmodes of the system. However, if one considers the spectrum of the system as a function of a perturbation that occurs in a direction that is not colinear with the laser propagation direction, the noise information is not contained entirely in the intensities of the measured optical modes.

The polarization dependence of EIT and EIA signals themselves are relatively well studied experimentally and theoretically [26–28] and EIT intensity noise spectroscopy in the propagation eigenbasis has been relatively well studied [16,17,19,20,23]. Little has been reported on the polarization dependence of EIT noise spectroscopy. Recent work using restricted sets of pre- [22] and post-cell [29] polarization basis choices could not obtain amplitude noise from experimental data due to the experimental protocols. It is clear in the preceding Refs. [22,29] that the authors understood the utility of the fact that post-cell polarization selection was not simply creating a linear combination of intensity noise correlations, but algebraically independent ones.

In Section 2 we summarize the experimental setup and protocol used. Section 3 describes the three level model used in this protocol and how it allows us to frame the experimental results in terms of noise in the underlying field amplitudes. We use the model to semi-quantitatively reproduce the experimentally measured $g^{(2)}(0)$ as a function of two-photon detuning in different (orthogonal) polarization bases. In Section 4 we test the amplitude noise hypothesis in a model independent way by first inverting experimentally measured intensity correlation data from three

OSA CONTINUUM

channels in a fixed basis to amplitude noise correlations. Then we use those computed amplitude noise correlations to generate intensity noise correlation statistics in other bases and compare directly with experimental measurements carried out in those other bases.

## 2. Experimental setup

The experimental setup is typical for the Zeeman EIT noise spectroscopy and is shown in Fig. 1. The EIT state is realized in a warm (44°C) enriched $^{87}$Rb buffer gas vapor cell (length = 8 cm), buffered with 10 Torr of Neon and Argon (5 Torr Ne + 5 Torr Ar ) by a linearly polarized beam from a free-running diode laser sent through the length of the cell. The linearly polarized input field (in our experiment, horizontal) has equal components $\sigma_+$ and $\sigma_-$ (right and left circularly polarized fields) of fixed phase. This light pumps atomic coherences between degenerate ground state Zeeman sub-levels, as in Hanle EIT. The degeneracy of the Zeeman sub-levels can be split by an applied longitudinal magnetic field. The amount of splitting $\Delta$ between the Zeeman sub-levels is determined by the strength of the applied magnetic field, and subsequently we refer to it as a the two-photon detuning. To ensure that a reproducible and stable splitting $\Delta$ is only a function of current applied to the solenoid around the vapor cell, it is magnetically shielded from the surrounding environment by three nested layers of $\mu$-metal magnetic shielding. (see [23] for more experimental details.)

The laser field is generated with a 795 nm free-running diode laser which is tuned via temperature and current modulation to the F=2 $\longrightarrow$ F'=1 hyperfine transition of the $^{87}$Rb D1 line. The diode laser's mean frequency is stabilized with a "loose-lock" to this hyperfine transition by an analog feedback circuit whose control signal is the saturated absorption signal from another rubidium cell. The laser's free-running linewidth of $\sim$ 80 MHz is unchanged by the loose-lock, which simply prevents long term laser frequency drift; there is no other frequency stabilization of the laser (e.g. no grating feedback - internal or external). The lock used in all the data collected and described here resulted in a modest negative (*i.e.* red) one-photon detuning of about 10 MHz. The large spectral bandwidth of such a "noisy" laser is desirable for EIT noise correlation studies. The large spectral bandwidth allows one to effectively probe many two photon pathways simultaneously. The residual intensity noise of the laser was measured to $\sim$ 0.2%, and this small amount of residual intensity noise does not affect the utility of the spectroscopic signal. [12,24,30] .

In the event that the perturbation (for example, an external magnetic field) is not colinear with the laser propagation direction, information about the perturbation on the system is contained in the both the magnitudes and (relative-) phase making up the amplitudes of the light fields, and noise spectroscopy of the optical mode amplitudes contains the spectral information of interest. If one knew a-priori the direction of the perturbation, one could calculate the optical polarization modes that correspond to the eigenmodes of the system and do standard intensity noise spectroscopy on those optical modes. If the direction of the system's perturbation is unknown, one must have a technique for measuring the amplitude noise of the light leaving the system. We accomplish this task by using the following technique.

Upon exciting the atomic vapor cell, the light is split into three different polarization components. For the two light fields from what we call the analyzer pair behind the PBS after the quarter wave plate, we compute the $g^{(2)}(0)$ using Eq. (1). Referring to Fig. (1)(a), most of the light (> 90%) is passed through a quarter wave-plate (QWP) before being split by a polarizing beam splitter (PBS) into linearly horizontal and vertical polarization components of what we refer to as the analyzer pair. When the QWP is aligned at 45° to the horizontal, one can view the QWP as transforming the right and left circular polarization to linear horizontal ($I_a$) and vertical ($I_b$) polarization intensities.

A small portion of the light ($\approx$ 8% for the third channel) is split off before the analyzer pair's quarter-wave plate via a glass window. The window is aligned at near normal incidence to

OSA CONTINUUM

leave the polarization state of both the transmitted and reflected light nearly unchanged. The polarization state incident to the analyzer pair optics is changed less than 1% by the pick-off window and all the optics prior to the analyzer pair. Similar to the analyzer pair light fields, the third channel light is passed through a QWP and a linear polarizer so that the intensity of light $I_c$ incident on the photodiode (see Fig. 1 and Eq. 2 ) corresponds to a fixed, algebraically independent amplitude combination (throughout this experiment, its QWP axis was rotated an additional 10° with respect to the orientation of the QWP before the analyzer pair that would have led to $\sigma_\pm$ there).

Selecting different polarization bases post-cell by rotating the quarter wave plate before the analyzer pair sends different linear combinations of the (assumed) underlying circular polarization field amplitudes to each of the channels $a$ and $b$. By simultaneously recording all three intensities, $I_a$ and $I_b$ and the third channel, $I_c$, we are able to determine all intensity noise correlations.

Each light intensity is measured on identical amplified silicon photodiodes whose output voltages are simultaneously digitized by a National Instruments 9223 and recorded in 4ms windows at a sampling rate of 1 MHz. This is done for different two-photon detunings (generated by the current in the solenoid). The amplified photodiode dark current noise power was spectrally flat (DC $\rightarrow$ 10 MHz) and varied between 2 to 12dB below the optical field's intensity noise of interest. A fixed bandpass filter was applied to all the sampled data to reduce technical noise. The filter parameters (frequency center and width) were chosen by requiring cross correlations between channels receiving identical polarizations be as close to one as practical (See also [31]).

## 3. Theory

The intensity cross correlation $g_2(0)$ (as defined above), while carefully studied in many earlier works, is only one of many possible independent and relevant correlation observables in these experiments. It is not possible to extract all the underlying amplitude noise spectra by measuring only the intensities $I_a$, $I_b$ and their fluctuations $\delta I_a$, $\delta I_b$ of the two circular polarization channels $\sigma_+$ and $\sigma_-$ emerging from the vapor cell. For example, passing the light emerging from the cell through a waveplate (delay $\tau$ at angle $\theta$) to the original input light's polarization gives the fluctuations $\delta I_c$ of $I_c$ (as in Fig. 1 modulo the overall efficiency of the sampling window),

$$\delta I_c = cos^2\theta \delta I_a + \sin^2\theta \delta I_b + 2\sin(2\theta)\cos(2\tau)\delta(ab_1) - 2\sin(2\theta)\sin(2\tau)\delta(ab_2), \tag{2}$$

where without loss of generality the real amplitudes $a, b_1, b_2$ represent the output fields making up $I_a = a^2$, $I_b = |b_1 + ib_2|^2$. Thus a third intensity channel, $I_c$, is added that measures light in a fixed, independent linear combination of amplitudes for $\sigma_+$ and $\sigma_-$. Clearly the full second-order correlation content of these light fields is encompassed by the six independent quantities $\langle\delta a\delta a\rangle, \langle\delta a\delta b_1\rangle, \langle\delta a\delta b_2\rangle, \langle\delta b_1\delta b_1\rangle, \langle\delta b_2\delta b_2\rangle$ and $\langle\delta b_1\delta b_2\rangle$. All intensity correlations can be built from these, for one example, $\langle\delta I_a\delta I_b\rangle = 16\delta a(b_1\langle\delta(ab_1)\rangle + b_2\langle\delta(ab_2)\rangle)$, where $\delta(ab_1) = a\delta b_1 + b_1\delta a$. Not surprisingly, although tedious to write down, the above transformation is invertible, indicating that the measurements of six intensity correlation functions between any three (amplitude algebraically independent) polarizations is expressible in terms of any other.

A three level atomic model quantitatively captures the noise properties of EIT amplitude and intensity correlations. (see, for example [16,23]). The theory model consists of a three-level $\Lambda$ system (ground states $|1\rangle$, $|2\rangle$ and excited state $|0\rangle$) (see Fig. 1(b)) with the output light's amplitudes receiving contributions from $\delta I_a \sim \Omega_-\rho_{20}$ and $\delta I_b \sim \Omega_+\rho_{10}$, where $\rho_{10} = |1\rangle\langle 0|$ is one of the usual density matrix elements. For reference, the Hamiltonian and Liouvillian for the system in Fig. 1(b) in the rotating frame is

$$H = D|0\rangle\langle 0| + (\Omega_+|0\rangle\langle 1| + \Omega_-|0\rangle\langle 2| + h.c.) - \frac{\Delta}{2}|1\rangle\langle 1| + \frac{\Delta}{2}|2\rangle\langle 2| \tag{3}$$

OSA CONTINUUM

$$
\begin{aligned}
\mathcal{L}\rho = & -\gamma_1|0\rangle\langle 0| - \gamma_2(|0\rangle\langle 1| + |0\rangle\langle 2| + h.c.) - \Gamma_1|1\rangle\langle 2| + \text{h.c.} \\
& -(|1\rangle\langle 1|(\Gamma - \Gamma\rho_{22}/\rho_{11} - \frac{\gamma}{2}\rho_{00}/\rho_{11}) - |2\rangle\langle 2|(\Gamma - \Gamma\rho_{11}/\rho_{22} - \frac{\gamma}{2}\rho_{00}/\rho_{22})
\end{aligned}
\tag{4}
$$

The key idea of the model is that since $\Gamma, \Gamma_1$ are so much smaller than $\gamma_1, \gamma_2$ (these are the population and coherence decay rates; refer to Fig. 1b), the coherence $\rho_{12}$ and the populations $\rho_{11}, \rho_{22}$ cannot evolve on the fast timescales indicated by the bandwidth of the laser, or even that of the recording bandwidth of the photodiode signals $I_a$ and $I_b$. Instead, $\rho_{11}, \rho_{22}, \rho_{12}$ only depend on $\bar{D} = \langle D\rangle$ (the average one-photon detuning) and $\bar{\Omega}_\pm = \langle\Omega_\pm\rangle$ (the Rabi frequencies of the input field written in terms of right $\sigma_+$ and left $\sigma_-$ circular polarization states) where here "$\langle\rangle$" refer to the time averaged value of those parameters. The noise we measure as the AC part of $I_a$ and $I_b$ then is entirely due to the changes in $\rho_{01}$ and $\rho_{02}$ (due to the changes in $D, \Omega_\pm$ consequent to the laser's phase noise and amplitude noise) inside the photodetection bandwidth.

As a further simplification, in practice we do not follow the rigorous time development of the $\rho_{01}, \rho_{02}$ in the optical Bloch equations,

$$\partial_t\rho = -i[H, \rho] + \mathcal{L}\rho \tag{5}$$

to compute the time average, but instead compute an ensemble average we henceforth denote by the same notation "$\langle\rangle$". The $\gamma \gg \Gamma$ timescales in the model allow us to consider the coherences $\rho_{01}$ and $\rho_{02}$ as results of Markov processes in the detunings $D$ and $\Omega_\pm$. Our ensemble thus consists of a flat distribution of $D$ about $\bar{D}$ that has a bandwidth larger than our photodetection of $I_a, I_b$ and $I_c$. Similarly, we assume that the distribution of $|\Omega_\pm|$ is flat and relatively narrow (less than a percent) about $\bar{\Omega}_\pm$, as indicated by experimental measurements and discussed in the preceding section. Thus we solve the steady state ($\partial_t\rho = 0$ in Eq. (5)) Bloch equations and assemble the theory predictions for the $I_a$ and $I_b$ and their correlators on that ensemble.

Note that there is no reason to expect one of these amplitude noise correlators to be significantly smaller than the others. Indeed, the model and our experimental data suggests that they are typically all within an order of magnitude of each other. Furthermore we note that we are not assuming Gaussian statistics. For example, experimental data and the theory model both indicate that there will be nonzero triple correlations of the AC parts of both amplitudes and intensities, but we do not focus on that here.

As mentioned above, in the experiment we simultaneously capture emerging optical field's intensity fluctuations in three (amplitude algebraically independent) polarizations allowing a straightforward, though tedious, recasting of the associated six two-intensity correlations $\langle\delta I_a\delta I_a\rangle, \langle\delta I_b\delta I_b\rangle, \langle\delta I_c\delta I_c\rangle, \langle\delta I_a\delta I_b\rangle, \langle\delta I_b\delta I_c\rangle, \langle\delta I_a\delta I_c\rangle$ into $\langle\delta a\delta a\rangle, \langle\delta a\delta b_1\rangle, \langle\delta a\delta b_2\rangle, \langle\delta b_1\delta b_1\rangle, \langle\delta b_2\delta b_2\rangle$, and $\langle\delta b_1\delta b_2\rangle$, giving a recording of the complete leading fluctuation correlation behavior at each value of the applied (longitudinal) magnetic field and one-photon detunings.

## 4. Experimental results and discussion

When the post-cell quarter wave plate is aligned at 45°, the measured noise correlation is between the $\sigma_+$ and $\sigma_-$, the propagation eigenstates for the EIT process. In this case, the contrast of $g^{(2)}(0)$ generally increases with power and its central feature eventually broadens. All the data shown here was taken at a lower optical power and larger beam diameter associated with the onset of the power broadening regime [23]. Rather than directly correlating the EIT Noise amplitude changes with externally applied magnetic field magnitudes and directions, we opt for a conceptually clearer and technically simpler test of our EIT amplitude noise model and experimental technique by understanding the EIT amplitude noise for a more general set of output polarization states (orthogonal elliptical instead of orthogonal linear) under a range of axial magnetic fields. We achieve this by rotating the post-cell quarter wave plate before the analyzer pair from its nominally 45° orientation with respect to the input polarization, we record systematic changes in the subsequently measured intensity correlation noise spectra in the analyzer detector

OSA CONTINUUM

pair. Each run then we are studying the scattering of the same input light states from the same atomic and magnetic states BUT using the different polarization bases as a way of reconstructing the rest of the statistical correlations in the light fields. As a function of the two-photon detuning $\Delta$, typical RMS noise traces in each port of the analyzer are shown in Fig. 2(a) and typical $g^{(2)}(0)$ from these data (points) and associated theory (lines) are shown in Fig. 2(b,c). We summarize our comparison between experiment and theory for EIT noise after a polarization basis change as follows:

1) **Shift:** For rotations of the QWP beyond 45°, the metrologically relevant central peak of $g^{(2)}(0)$ is no longer at zero two-photon detuning. The direction and magnitude of the shift is well accounted for in the three level atomic model, [16,23]. For rotations of the post-cell quarter wave plate beyond its nominal 45° orientation we show in Fig. 3(a) the shift and width of the $g^{(2)}(0)$ as a function of additional rotation beyond 45°. Although we have not included it here, the shift of the peak with power at fixed angle is also well modeled with the theory model. Also, as expected, the signs of the shift and the asymmetry (described below) flip with the sign of the one photon detuning.

2) **Asymmetry:** When the QWP is at the nominal 45° rotation, $g^{(2)}(0)$ is symmetric in the two-photon detuning. For rotations of the QWP beyond 45°, $g^{(2)}(0)$ becomes asymmetric, and so we define the asymmetry $\upsilon = \frac{W_+ - W_-}{W_+ + W_-}$ where the unsigned half-widths $W_\pm$ are the magnitudes of the detunings at which the $g^{(2)}(0)$ crosses zero. Figure 3(b) is a plot of $\upsilon$ for both experiment (dots) and theory (lines). The theory further indicates that the sign of

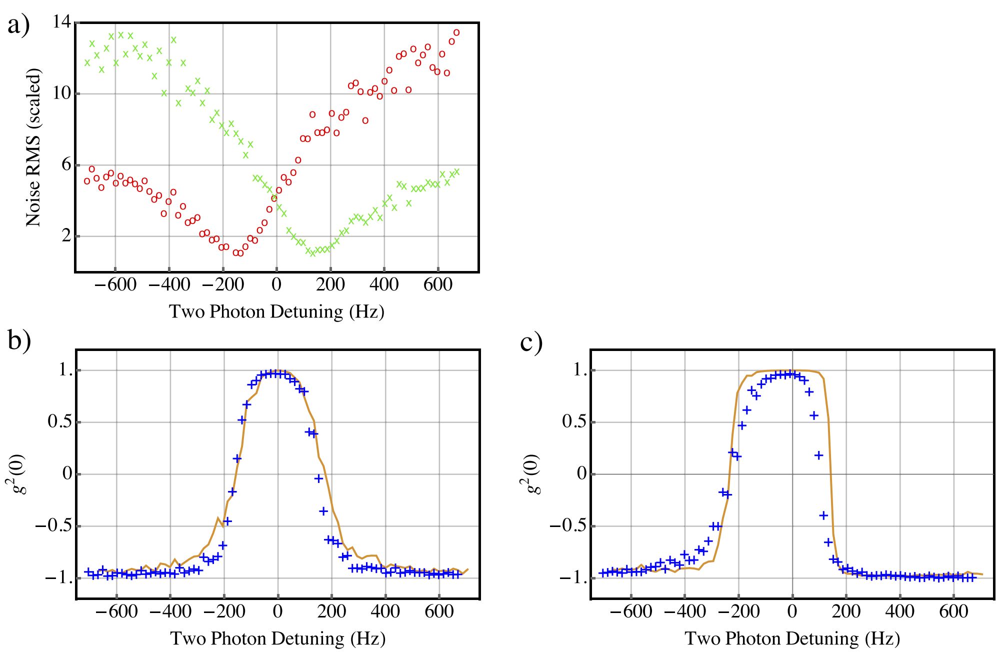


**Fig. 2.** (a) Experimental RMS noise in each of the analyzer ports as a function of the two-photon detuning with the post-cell phase plate held at 45° ($\sigma_+$ in Red ∘'s, and $\sigma_-$ in green x's). (b) The cross-correlation statistic, $g^{(2)}(0)$ versus detuning measured (points) and theory (line) for the cross-correlation statistic for the post-cell phase plate held at 45° and (c) Experiment (points) and theory (line) for the post-cell quarter wave plate held at 60°. The lack of smoothness of the theory curves is due to finite sample size for each detuning (here chosen to match that of the experimental data)

the asymmetry should flip with the sign of the angle of the quarter wave plate orientation beyond 45° degrees, an effect that was experimentally verified but has not been separately quantified. The fit parameters used for this comparison between theory and experiment are the total ground state decoherence rate and the optical power, fixed by data from only the 45° quarter wave plate orientation.

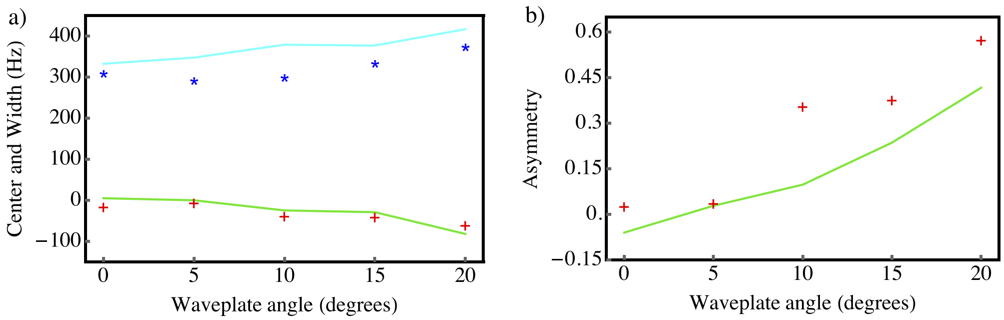


**Fig. 3.** (a) Shift of the $g^{(2)}(0)$ maxima, experiment (red +'s) and theory (green line) with wave plate angle beyond 45° degrees. Also shown is the FWHM, experiment (blue *'s) and theory (cyan line). (b) The asymmetry $\upsilon$, experiment (red +'s) and theory (green line), as a function of the wave plate angle beyond 45° degrees.

The favorable comparison between theory (lines) and experiment (points) in Fig. 2b,c and Fig. 3 amount to another test of the aforementioned theory model for the amplitude noise correlators since they depend non-trivially on experimental parameters (optical detunings and longitudinal magnetic field) that cannot be reduced to some simple structural change associated with the choice of final state polarization measurement basis.

## 5. Conclusions

We have tested an approach to understanding intensity noise spectra from an EIT system as a Markov process in the one-photon detunings of a single input light field amplitude. Our results indicate that one can reliably compute EIT intensity noise correlations in an arbitrary polarization basis by identifying a set of amplitude noise correlations in a given polarization basis. Since vector magnetometers detect the transverse components of a magnetic field through changes in the ellipticity of the light fields, the tests performed here suggest a new way of using EIT noise protocols in vector atomic vapor magnetometry and indicate potential utility and robustness of using noise spectroscopy in device applications such as atomic clocks [32] and magnetometers [33].

## Funding

National Science Foundation (DMR-1609077, PHY-1506499).

## Acknowledgements

We are grateful to I. Novikova, Y. Xiao, D. Phillips and R. Walsworth for discussions and equipment use.

## Disclosures

The authors declare no conflicts of interest.

OSA CONTINUUM

## References


1. M. Fleischhauer, A. Imamoglu, and J. Marangos, "Electromagnetically induced transparency: Optics in coherent media," Rev. Mod. Phys. **77**(2), 633–673 (2005).
2. M. D. Lukin, "*Colloquium* : Trapping and manipulating photon states in atomic ensembles," Rev. Mod. Phys. **75**(2), 457–472 (2003).
3. C. H. van der Wal, M. D. Eisaman, A. Andre', R. L. Walsworth, D. F. Phillips, A. S. Zibrov, and M. D. Lukin, "Atomic Memory for Correlated Photon States," Science **301**(5630), 196–200 (2003).
4. L.-M. Duan, M. Lukin, J. I. Cirac, and P. Zoller, "Long-distance quantum communication with atomic ensembles and linear optics," Nature **414**(6862), 413–418 (2001).
5. J. Vanier, "Atomic clocks based on coherent population trapping: a review," Appl. Phys. B **81**(4), 421–442 (2005).
6. D. Budker and M. Romalis, "Optical magnetometry," Nat. Phys. **3**(4), 227–234 (2007).
7. E. Knill, R. Laflamme, and G. J. Milburn, "A scheme for efficient quantum computation with linear optics," Nature **409**(6816), 46–52 (2001).
8. T. Yabuzaki, T. Mitsui, and U. Tanaka, "New type of high-resolution spectroscopy with a diode laser," Phys. Rev. Lett. **67**(18), 2453–2456 (1991).
9. D. H. McIntyre, C. E. Farichild, J. Cooper, and R. Walser, "Diode-laser noise spectroscopy of rubidium," Opt. Lett. **18**(21), 1816–1818 (1993).
10. M. Rosenbluh, A. Rosenhouse-Dantsker, A. D. Wilson-Gordon, M. D. Levenson, and R. Walser, "Spectroscopy with diode-laser noise," Opt. Commun. **146**(1-6), 158–162 (1998).
11. D. Felinto, L. S. Cruz, R. A. de Oliveira, H. M. Florez, M. H. G. de Miranda, P. Nussenzveig, M. Martinelli, and J. W. R. Tabosa, "Physical interpretation for the correlation spectra of electromagnetically-induced-transparency resonances," Opt. Express **21**(2), 1512–1519 (2013).
12. P. Li, L. Feng, and Y. Xiao, "Resolving multiple peaks using a sub-transit-linewidth cross-correlation resonance," Phys. Rev. A **89**(4), 043835 (2014).
13. S. Rao, X. Hu, J. Xu, and L. Li, "Optical switching of cross intensity correlation in cavity electromagnetically induced transparency," J. Phys. B: At., Mol. Opt. Phys. **50**(5), 055504 (2017).
14. J. Camparo and J. Coffer, "Conversion of laser phase noise to amplitude noise in a resonant atomic vapor: The role of laser linewidth," Phys. Rev. A **59**(1), 728–735 (1999).
15. R. Walser and P. Zoller, "Laser-noise-induced polarization fluctuations as a spectroscopic tool," Phys. Rev. A **49**(6), 5067–5077 (1994).
16. Y. Xiao, T. Wang, M. Baryakhtar, M. Van Camp, M. Crescimanno, M. Hohensee, L. Jiang, D. F. Phillips, M. D. Lukin, S. F. Yelin, and R. L. Walsworth, "Electromagnetically induced transparency with noisy lasers," Phys. Rev. A **80**(4), 041805 (2009).
17. V. A. Sautenkov, Y. V. Rostovtsev, and M. O. Scully, "Switching between photon-photon correlations and Raman anticorrelations in a coherently prepared Rb vapor," Phys. Rev. A **72**(6), 065801 (2005).
18. M. Martinelli, P. Valente, H. Failache, D. Felinto, L. S. Cruz, P. Nussenzveig, and A. Lezama, "Noise spectroscopy of nonlinear magneto-optical resonances in Rb vapor," Phys. Rev. A **69**(4), 043809 (2004).
19. L. S. Cruz, D. Felinto, J. G. Aguirre-Gomez, M. Martinelli, P. Valente, A. Lezama, and P. Nussenzveig, "Laser-noise-induced correlations and anti-correlations in electromagnetically induced transparency," Eur. Phys. J. D **41**(3), 531–539 (2007).
20. G. O. Ariunbold, Y. V. Rostovtsev, V. A. Sautenkov, and M. O. Scully, "Intensity correlation and anti-correlations in coherently driven atomic vapor," J. Mod. Opt. **57**(14-15), 1417–1427 (2010).
21. L. Feng, P. Li, L. Jiang, J. Wen, and Y. Xiao, "Coherence-Assisted Resonance with Sub-Transit-Limited Linewidth," Phys. Rev. Lett. **109**(23), 233006 (2012).
22. H. J. Lee and H. S. Moon, "Intensity correlation and anti-correlation in electromagnetically induced absorption," Opt. Express **21**(2), 2414–2422 (2013).
23. A. Zheng, A. Green, M. Crescimanno, and S. O'Leary, "EIT Intensity Correlation Power Broadening in a Buffer Gas," Phys. Rev. B **93**(4), 043825 (2016).
24. H. M. Florez, L. S. Cruz, M. H. G. de Miranda, R. A. de Oliveira, J. W. R. Tabosa, M. Martinelli, and D. Felinto, "Power-broadening-free correlation spectroscopy in cold atoms," Phys. Rev. A **88**(3), 033812 (2013).
25. H. M. Florez, C. González, and M. Martinelli, "Perturbative approach in the frequency domain for the intensity correlation spectrum in electromagnetically induced transparency," Phys. Rev. A **94**(1), 012503 (2016).
26. A. V. Taichenachev, A. M. Tumaikin, and V. I. Yudin, "Invariant treatment of coherent population trapping in an elliptically polarized field," Europhys. Lett. **45**(3), 301–306 (1999).
27. K. Nasyrov, S. Cartaleva, N. Petrov, V. Biancalana, Y. Dancheva, E. Mariotti, and L. Moi, "Coherent population trapping resonances in Cs atoms excited by elliptically polarized light," Phys. Rev. A **74**(1), 013811 (2006).
28. D. V. Brazhnikov, A. V. Taichenachev, A. M. Tumaiken, V. I. Yudin, S. A. Zibrov, Y. O. Dudin, V. V. Vasil'ev, and V. L. Velichansky, "Features of Magneto-Optical Resonances in an Elliptically Polarized Traveling Light Wave," JETP Lett. **83**(2), 64–68 (2006).
29. H. J. Lee, T. Jeong, and H. S. Moon, "Postselection of a polarization basis in intensity correlations under electromagnetically induced transparency," Phys. Rev. A **90**(3), 033843 (2014).

OSA CONTINUUM

30. T.-C. Zhang, J.-P. Poizat, P. Grelu, J.-F. Roch, P. Grangier, F. Marin, A. Bramati, V. Jost, M. D. Levenson, and E. Giacobino, "Quantum noise of free-running and externally-stabilized laser diodes," Quantum Semiclassical Opt. **7**(4), 601–613 (1995).
31. T. Jeong, I. H. Bae, and H. S. Moon, "Noise filtering via electromagnetically induced transparency," Opt. Commun. **383**, 31–35 (2017).
32. J. Kitching, H. G. Robinson, L. Hollberg, S. Knappe, and R. Wynands, "Optical-pumping noise in laser-pumped, all-optical microwave frequency references," J. Opt. Soc. Am. B **18**(11), 1676–1683 (2001).
33. P. D. D. Schwindt, S. Knappe, V. Shah, L. Hollberg, J. Kitching, L.-A. Liew, and J. Moreland, "Chip-scale atomic magnetometer," Appl. Phys. Lett. **85**(26), 6409–6411 (2004).